ELSEVIER

Temperature variability in the tropical mesosphere during the northern hemisphere winter

M.G. Shepherd [a,*], D.L. Wu [b], I.N. Fedulina [c], S. Gurubaran [d]

[a] *Centre for Research in Earth and Space Science, York University, 4700 Keele Street, Toronto, Ont., Canada M3J 1P3*
[b] *Microwave Atmospheric Science, M/S 183-701, 4800 Oak Grove Drive, JPL/Caltech, Pasadena, CA 91109, USA*
[c] *Institute of Ionosphere, Kamenskoe Plato, Almaty 480020, Kazakhstan*
[d] *Equatorial Geophysical Research Laboratory, Indian Institute of Geomagnetism, Krishnapuram, Tirunelveli 627 011, India*

Abstract

Temperature observations at 20–90 km height and 5°N–15°N during the period of December 1992–March 1993 from the WINDII and MLS experiments on the UARS satellite are analysed together with MF radar winds and UKMO assimilated fields of temperature and zonal and meridional winds. The correlation between the different datasets at the tropics and zonal mean wind data at mid latitudes is examined for period February–March 1993, when series of stratospheric warming events were observed at middle and high latitudes. Wavelet analysis is applied to investigate coupling between stationary and travelling planetary waves in the stratosphere and the upper mesosphere. Planetary waves $m = 1$ with periods of 4–7 days, 8–12 days and 13–18 days are found to dominate the period. Westward 7- and 16–18 day waves at the tropics appear enhanced by stationary planetary waves during sudden stratospheric warming events.
© 2007 COSPAR. Published by Elsevier Ltd. All rights reserved.

Keywords: Temperature; Zonal winds; Tropical mesosphere; Stratospheric warming

1. Introduction

There are numerous studies of the effects of sudden stratospheric warmings (SSW) on the dynamics of the upper mesosphere and the mesosphere/lower thermosphere (MLT) region at high and mid-latitudes (e.g., Quiroz, 1969, 1971; Labitzke, 1972; Hirota and Barnett, 1977; Gregory and Manson, 1975; Whiteway and Carswell, 1994; Walterscheid et al., 2000; Hoffmann et al., 2002; Cho et al., 2004; Manson et al., 2006). It has been shown that events with sudden increase of the temperature in the stratosphere affect the zonal wind field in the stratosphere and are associated with cooling of the mesosphere. Temperature variability similar to the variability observed in the middle and high-latitude stratosphere and MLT region during SSW has also been observed at the tropics (Fritz and Soules, 1970; Mukherjee and Ramana Murty, 1972; Mukherjee et al., 1987; Sivakumar et al., 2004; Kodera, 2006). Examining the radiance measurements from the Nimbus 3 satellite Fritz and Soules (1970) were the first to show that the perturbations in the stratosphere at the higher latitudes are related to those at the tropics. The SSW at high latitudes was accompanied by simultaneous cooling in the tropical stratosphere and in the summer hemisphere. The amplitude of the temperature changes observed is larger at high and middle latitudes than at the tropics and in the summer hemisphere.

Recently, Sivakumar et al. (2004) examined Rayleigh lidar temperature observations from Gadanki (13.5°N, 79.2°E) for possible SSW effects on the tropical stratosphere and lower mesosphere. They reported a SSW event at low latitudes about a week after a major stratospheric warming was registered at high latitudes, with a temperature increase at 45 km height of ∼18 K above the winter mean values.

---

* Corresponding author.
E-mail address: mshepher@yorku.ca (M.G. Shepherd).

The equatorial and tropical middle atmosphere is also the host of such phenomenon as the quasi-biennial oscillation (QBO) (Baldwin et al., 2001), whose effects have also been observed at middle and high latitudes (e.g., Gray et al., 2001 and references therein). It has been suggested that the QBO can trigger the SSW events (Labitzke, 1987). Studies on the interannual variability of the SSW have shown that more major stratospheric mid-winter warmings occurred in the easterly phase of the stratospheric QBO and that the relatively few major mid-winter warmings observed in the westerly phase of the QBO took place only when the sunspot number was high. These results suggest that the QBO influences the cooling in the polar MLT region associated with the SSW (Labitzke, 1987).

The purpose of this study is to examine the SSW effects on the tropical (low latitude) mesosphere employing satellite temperature observations from the Wind Imaging Interferometer (WINDII) (Shepherd et al., 1993) and the Microwave Limb Sounder (MLS) (Barath et al., 1993) experiments on the Upper Research Satellite (UARS) (Reber et al., 1993) combined with ground-based MF radar (MFR) zonal and meridional winds from Tirunelveli (8.7°N, 77.8°E) and UK Meteorological Office (UKMO) assimilated field data. As the MFR winds are obtained at a site very close to those used in the work of Mukherjee and Ramana Murty (1972); Mukherjee et al. (1987) and Sivakumar et al. (2004), together with the satellite observations at the 5°N–15°N latitude range it is possible to compare the global pattern of the winter middle atmosphere observed by the satellites and the local variability seen in the ground-based observations. The results reported here are a part of a more extended study on the stratospheric warming effects on the tropical mesosphere (Shepherd et al., 2007) and concentrate on the period from December 1992 to March 1993.

2. Observations

2.1. WINDII temperature data

The WINDII temperature data are derived from the solar Rayleigh scattering radiances observed at the limb by the atomic oxygen green line background filter at a wavelength of 553 nm. The retrieval procedure and the data validation have been discussed elsewhere (Shepherd et al., 2001, 2004). The WINDII daytime temperatures from November 1991 to April 1997 provide global coverage from 50°S to 72°N over an altitude range from 65 km to 115 km. Orbital constraints and instrument viewing geometry limit WINDII global coverage between yaw periods from 42° in one hemisphere to 72° in the other and the reverse as a yaw of the satellite takes place approximately every 36 days. Thus the latitude range of ±42° is viewed around the equator all the time independently of the yaw. The satellite orbit precesses at a rate of 5° day^{-1}, which is equivalent to a change in local time by 20 min/day

at given latitude. The most regular WINDII temperature observations were for the period of January 1992–April 1994 and January 1995–April 1997. An earlier study of the seasonal variability of the mesospheric temperatures at the tropics by Shepherd et al. (2005) has shown its relationship with the zonal wind variability at the same latitudes, as well as the effect of the QBO on this variability.

For the purpose of the present study the WINDII temperature data from December 1992 to March 1993 are binned in a 10° latitude band of 5°N–15°N to provide daytime daily zonal mean values in the height range from 70 km to 95 km. Each daily zonal mean value corresponds to the mean local time at which the satellite orbit crossed the 10° latitude bin and thus contains the tidal contribution at that particular local time.

2.2. MLS temperature data

The MLS temperatures (Wu et al., 2003) in the height range of 20–90 km analyzed here are derived from the MLS O_2 emissions at 63 GHz. The estimated precision of the MLS temperatures varies from 1.5 K to 4 K between 20 km and 60 km, 6–8 K between 60 km and 85 km and increases sharply above 90 km. Comparisons with other datasets suggest biases at some altitudes, particularly above 80 km but these are not expected to significantly affect the temperature variations that will be examined here. The MLS latitude coverage on a given day is from 34° in one hemisphere to 80° in the other. Similarly to WINDII, the latitude range of ±34° around the equator is near-continuously observed by MLS independently of the yaw. In the current study we use MLS daytime temperature data for the same period of interest as WINDII, namely December 1992–March 1993 for consistency in the results obtained and their interpretation. The data are also binned in a 10° latitude band of 5°N–15°N and provide daytime daily zonal mean values for the height range 20–90 km. Strictly speaking WINDII and MLS do not look at the same volume of air at the same time since the WINDII field of view (FOV) is at 45° from the UARS orbit track (the WINDII temperatures are retrieved from FOV1 observations), while MLS looks at 90° to it. However, as we consider daily zonal mean values the differences are expected to be negligible. For consistency with the WINDII observations only MLS daytime observations are selected and analysed.

2.3. MF radar wind data

Mesospheric wind data obtained from the partial reflection radar operating at Tirunelveli (8.7°N, 77.8°E) have also been used for the period of December 1992–February 1993. The radar system operating at 1.98 MHz is identical to the one placed on Christmas Island by the University of Adelaide (Rajaram and Gurubaran, 1998; Vincent and Lesicar, 1991) for more details on the system]. The wind observations cover the altitude range from 70 km to 98 km and are daily mean values obtained from 1 h-aver-

aged data accumulated on a daily basis. At altitudes above 80 km the wind measurements cover a full 24-h cycle, while the datasets below 80 km may have some of the hourly slots unfilled during night hours giving a rise of the standard deviation of the data from $0.2 \, ms^{-1}$ above 82–84 km to as much as $3 \, ms^{-1}$ at the bottom of the radar altitude range during winter (Rajaram and Gurubaran, 1998). As the data extend over the 24-h diurnal cycle the daily-mean values obtained above 80 km are practically free of tidal influence.

2.4. UKMO data

We have also used stratospheric fields of daily (at 12:00 UTC, Coordinated Universal Time) temperature, zonal and meridional wind components provided by the UK Meteorological Office (UKMO) from the British Atmospheric Data Centre (BADC) website at http://badc.nerc.ac.uk. These data have global coverage with 2.5° latitudinal and 3.75° longitudinal steps and are available for 22 pressure levels from 1000 hPa to 0.316 hPa ($\sim$0–55 km). The description of the original data assimilation system is in Swinbank and O'Neill (1994a) and of the new (November 2000) three-dimensional variational (3D-VAR) system in Swinbank and Ortland (2003). In the current study we employ zonally averaged data at 1 hPa pressure level ($\sim$45 km) over the latitude band of 7.5°N, 10°N, and 12.5°N, centred at 10°N, for the periods of October 1992–April 1993. The UKMO analyses well represent the major features of atmospheric circulation (Swinbank and O'Neill, 1994b; Orsolini et al., 1997). Systematic errors in the model are reported to be small except near the upper boundary where they are attributed to shortcomings of the parameterizations of gravity-wave drag and radiation.

2.5. Data analysis

For the purpose of the current study the datasets considered have been subjected to standard spectral analysis including the Lomb-Scargle periodogram (Scargle, 1982; Hocke, 1998) and Morlet wavelet (Torrence and Compo, 1998). The analysis was carried our separately for the mesosphere and stratosphere with a sampling grid of 1-day resolution. The wavelet approach allows the decomposition of the time series into time-frequency space thus determining both the constituent frequencies and how these frequencies vary with time, producing a two-dimensional time-frequency image (e.g., Torrence and Compo, 1998). In the stratosphere the analysis of the UKMO assimilated data fields employed a more complex method of data processing described by Fedulina et al. (2004) as the data are examined for stationary and travelling (westward and eastward) planetary waves with zonal wave-number $m = 1$ and $m = 2$.

One problem with the wavelet transform is that it requires regularly spaced data points in the time series under consideration, i.e., there should be no gaps in the data. The gaps in the time series considered here were filled with a linear interpolation between the neighbouring data points. While this prevents the time series from a discontinuity which otherwise could be interpreted by the wavelet as a legitimate periodicity it does not introduce new spectral characteristics to the experimental dataset and therefore preserves the original planetary wave spectra.

3. Results

The dynamics of the winter mesosphere (November–February) is marked by considerable gravity wave activity and events of SSW, which in turn are coupled with planetary wave activity in the mesosphere and appear as cold temperature anomalies. As was first described by Matsuno (1971) (see also Andrews et al., 1987) the key mechanism for the generation of stratospheric warming is the growth of upward propagating planetary waves from the troposphere and the interaction between the transient wave and the mean flow. In a modelling study employing the TIME-GCM Liu and Roble (2002) have shown that this interaction decelerates and/or reverses the westerly winter stratospheric jet and induces a downward circulation in the stratosphere and upward circulation in the mesosphere, which in turn lead to adiabatic warming/cooling in the stratosphere/mesosphere, respectively. An essential ingredient in this mechanism is the amplification of planetary waves and the planetary wave interaction with the mean flow. The main mechanism for planetary wave amplification is considered to be the resonant wave (wave 1 and wave 2) amplification under winter conditions (Liu and Roble, 2002, and the references therein).

The winter of 1992–1993 was one in a series of 7 consecutive winter seasons in the 1990s (1991–1998) when no major SSW were observed (Labitzke and Naujokat, 2000). However, in February and early March 1993 a series of SSW was observed at high latitudes on February 3, 18, 26 and March 8 (Day 400, 415, 423 and 433, respectively, if counted from January 1 1992) (e.g., Whiteway and Carswell, 1994; Walterscheid et al., 2000; Hoffmann et al., 2002). In the mesosphere at mid-latitudes, at 55°N, SSW events were observed on December 22, 1992, February 16, and March 6, 1993 (Day 357, 413, and 431) (Hoffmann et al. (2002), their Table 2). From these, the SW event on February 16 (Day 413) 1993 was determined as a minor SW. According to Labitzke and Naujokat (2000) (see also Hoffmann et al., 2002) the minor SSW are defined as "a significant temperature increase (at least 25 K per week) at any stratospheric level in any area of the wintertime hemisphere. They can be intense and sometimes also reverse the temperature gradient, but they do not result in the reversal of the circulation at the 10 hPa level".

With this in mind we have examined the MFR zonal wind field observed at tropical latitudes, at Tirunelveli (8.7°N), during the period of December 1992–February 1993 and in the altitude range from 70 km to 98 km, as shown in Fig. 1. The MFR zonal winds display what would
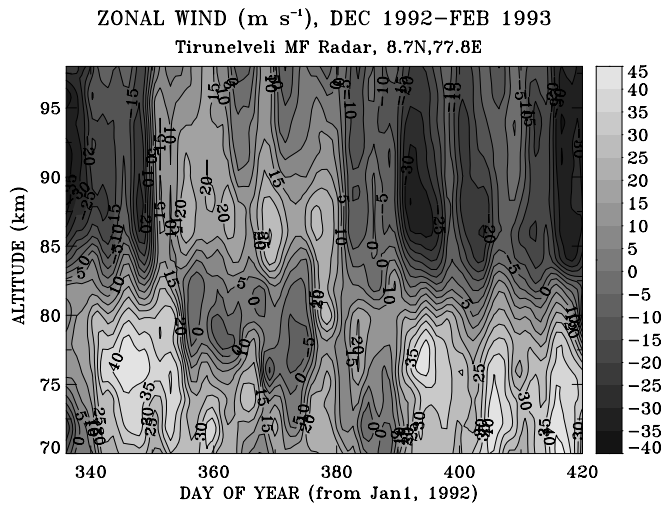
Fig. 1. Height–time cross section of mesospheric daily mean zonal wind velocity observed at Tirunelveli at 8.7°N over the period from December 1992 to February 1993.

be considered a typical tropical mesosphere winter wind structure with strong westerly winds extending up to 82–85 km height, and reversing to prevailing easterly winds above that height, if it was not for the perturbation seen between Day 356 and 390 (December 21, 1992–January 24, 1993). There appears to be a deceleration of the daily mean westerly zonal wind extending from 70 km to 84 km. A strong wind shear is observed at ~77–82 km around Day 350–355 (December 15–21, 1992) when the wind speed decreased from 40 ms^{-1} to -5 ms^{-1} within 2–3 days and stayed weak and easterly over a period of about a month (till Day 390, January 24, 1993), before reversing again to its normal winter westerly pattern. However, wind reversal from 83 to 98 km started earlier (around Day 352) than in the lower altitude (around Day 356). There is a downward progression that can be traced both in the easterly winds starting at ~90 km height on Day 335 and ending at 70 km on Day 390 or in the westerly winds – starting at about ~90 km height on Day 355–360 and ending on Day 415 at 70 km. The rate of the descent is 0.35 km day^{-1} suggesting upwelling during the period of day 355–380 with the same rate. Some further acceleration of the easterly winds at ~87 km is also observed at the end of January–early February (~Day 392–400) and February 21 (Day 418), 1993, with maximum wind speed of -35 ms^{-1}. Both signatures are accompanied by strong westerly winds below 80–82 km height. The wind reversal observed around Day 356 coincides in time and shows similarities in pattern with an event on December 22, 1992 (Day 357) when an enhanced heat flux, an enhancement of height wave 2 and a reversal of the zonal mean flow at 1 hPa and in the lower mesosphere was observed at 55°N (Hoffmann et al., 2002, Table 2). The wind perturbations around Day 397–400 and Day 418 appear very close in time to the SSW event registered on Day 413 (February 16, 1993) in the mesosphere and on Day 400 (February 3, 1993) at 10 hPa at 55°N. Since the available MFR wind data do

not extend beyond Day 420 (February 23, 1993) we cannot examine further this wind pattern.

The mesospheric temperature field observed by WINDII and expressed in terms of daily zonal mean temperatures over the latitude range of 5°N–15°N, for December 1992–March 1993 is shown in Fig. 2. A temperature cooling of the order of 7 K below the mean value (192 K) can be seen at 84–85 km beginning from Day 360 (December 25, 1992) until about Day 385 (January 19, 1993) before descending and forming a second cold anomaly (defined as a departure from the climatological mean) at ~78 km on Day 397 (January 31, 1993). The descent of 7 km between the two WINDII temperature anomalies, seen in Fig. 2, has a good correspondence with the easterly zonal wind signature during the same period below 85 km, shown in Fig. 1. However the temperature anomaly appears 5 km higher than the signature in the easterly winds. Unfortunately, there are no WINDII temperature observations between Day 397 and Day 410 which makes it impossible to determine the peak date of that anomaly in the WINDII observations. Hoffmann et al. (2002) show that the SSW on February 3, 1993 caused a reversal of the meridional temperature gradient at 10 hPa, but no other signatures were observed, thus appearing unlikely for this perturbation to have propagated equator-ward to ~10°N from its origin, both meridionally and vertically. There is also a good correspondence between the cold temperature anomalies around Day 395–397 and ~Day 420 (January 29–31 and February 23, 1993) and the MFR increased easterly winds above 80 km observed around Day 397 and Day 420. The downward propagation of the cold temperature anomaly and, for that matter the easterly (or westerly) zonal wind, as shown in Fig. 1 suggests an up-welling and adiabatic cooling, consistent with the effects which the interaction of a transient planetary wave with the stratospheric jet would have on the mesosphere (Liu and Roble, 2002).
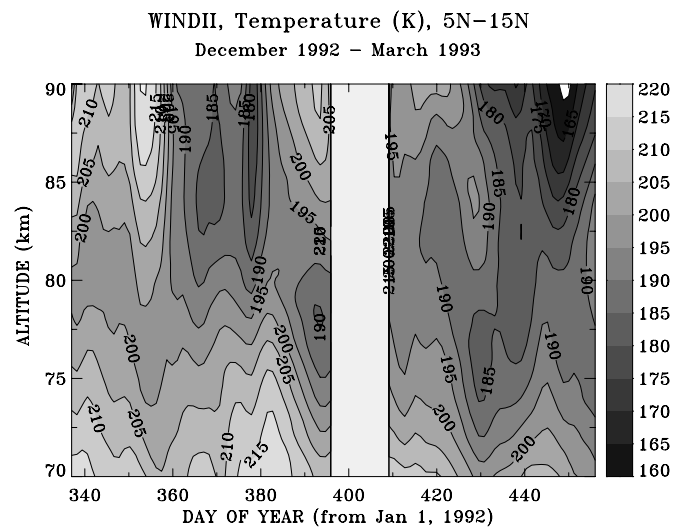
Fig. 2. Height–time cross section of mesospheric temperatures observed by WINDII over the period from December 1992 to April 1993.

The other two SSW events identified by Hoffmann et al. (2002), on February 26, 1993 and March 8, 1993 (Day 423 and 433, respectively) appear to be well within the period of the cold temperature anomaly (Day 415–445) (Fig. 2) with downward progression of about 1 km/day and temperature difference of ∼10 K at 78 km. These temperature anomalies extend further both vertically and in time into the cold temperature anomaly associated with coupling of the QBO and the semi-annual oscillation (SAO) at these latitudes and at equinox, as was discussed at length by Shepherd et al. (2005). Unfortunately, there are no zonal wind data from Day 420 (February 23, 1993) to Day 456 (March 31, 1993), although the monthly mean altitude cross section indicates the correspondence between the cold temperature anomalies and the easterly phase of the mesospheric zonal wind (e.g., Shepherd et al., 2005, Fig. 8).

To examine the source of the perturbations observed the analysis is further extended to temperature data from the MLS experiment for the same period over the height range from 20 km to 90 km. Fig. 3 gives the height–time cross section of the temperature field as observed by the MLS experiment in the upper mesosphere, 70–90 km, (Fig. 3a) and stratosphere and lower mesosphere, 30–70 km (Fig. 3b). There is a good agreement between the WINDII and the MLS daytime observations around Day 360–380 and Day 420–440, although the MLS amplitudes are relatively smaller. There are cold anomalies which descent to ∼70 km, indicating weak temperature inversions with minima between 72 km and 80 km. The cold anomaly around Day 435–440 (March 10–15, 1993) appears deeper with larger temperature gradients than the anomaly following December solstice (Day 360–370). As these are only daytime observations they are inevitably biased by the diurnal tide and thus the temperature inversions and cold anomalies could easily be assumed as tidal signatures resulting from changes in the local time (e.g., Meriwether et al., 1998). Fig. 4 gives the change of local time (LT) for WINDII and MLS during the period of interest. The LT changes by 12 h (half of the diurnal cycle) between Day 358 and 385, which includes the first temperature anomaly observed both in WINDII and MLS. There is another 12-h difference in LT between Days 397–423 (January 31–February 23, 1993) and finally – a 9-h change of LT during the time of the second cold temperature anomaly of Day 431–445 (March 6–March 20, 1993). According to Forbes and Wu (2006) the amplitude of the diurnal and semidiurnal tides for January are of the order of 4.5 K and 2.4 K, respectively. Thus the most we can expect as a change due to the tidal bias is only the half of these amplitudes over the 12-h period (2.2 K and 1.2 K), which is still less than the variability observed during the Day 350-380 perturbation.

The second cold anomaly seen around Day 420–450, both by WINDII and MLS was also investigated by Shepherd et al. (2005). In that study the WINDII temperatures for March–April 1993 were corrected for tidal contribution using the tidal parameters of Forbes and Wu (2006)
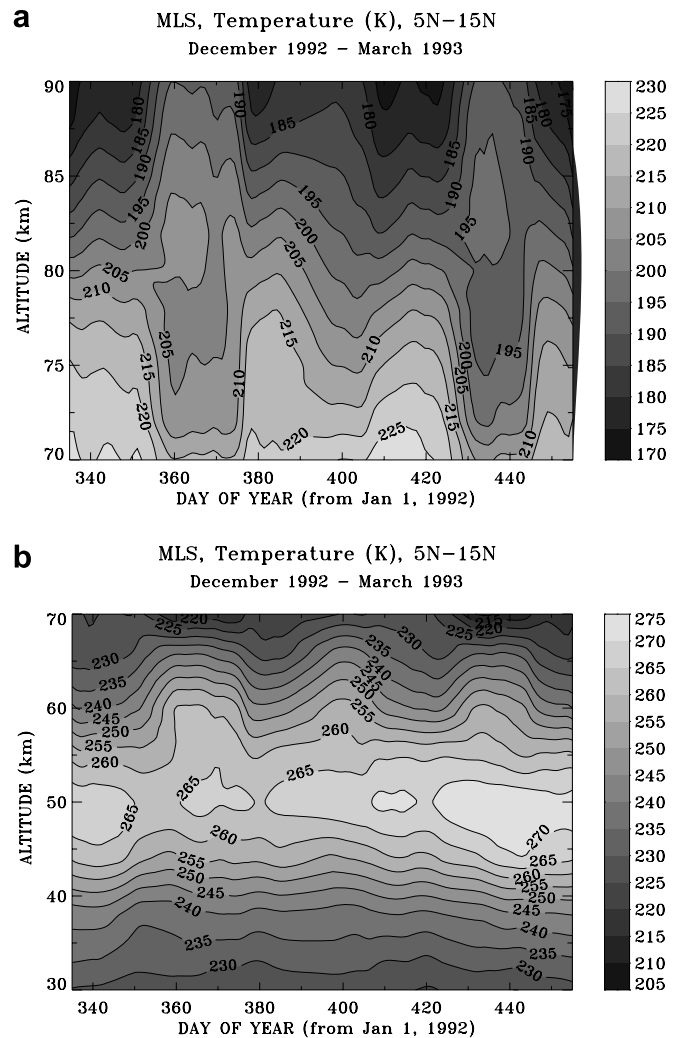
Fig. 3. Daily-mean zonal temperatures from MLS in an altitude-height section at 5°–15°N and from December 1, 1992 to March 31, 1993 at: (a) 70–90 km height, and (b) 30–70 km height.
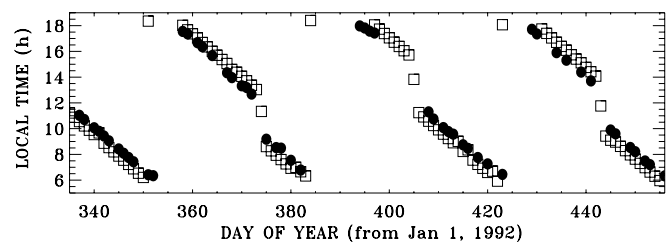
Fig. 4. Local time sampling for WINDII (solid circles) and MLS (squares) from December 1992 to March 1993 (Day 335–Day 456).

obtained from the MLS temperature observation. Even after the correction the amplitude of the cold temperature anomaly around Day 425–450 (March 1–25, 1993) was still of the order of 10–15 K (Shepherd et al., 2005, Their Fig. 2a). This perturbation preceded a deep cold temperature anomaly identified as a signature of the coupling of the SAO with the QBO at these latitudes and resulting from the residual circulation. In the stratosphere the cold anomaly corresponds to a period of increased stratospheric

temperatures around 47 km (Fig. 3b), where the strato-sphere is about 5–10 K warmer then the earlier period. Although there is no MFR wind observations from Tirun-elveli for this time, zonal wind observations by the High Resolution Doppler Imager (HRDI) (Lieberman and Riggin, 1997) indicate a strong zonal wind shear in the mesosphere during a reversal from westerly to easterly winds at the time of the cold temperature anomaly seen both by WINDII and MLS (Figs. 2 and 3a).

To provide an estimate on the degree of correspondence between the perturbations observed in the tropical temperature and wind fields with those seen in the zonal wind at 55°N we apply cross-correlation analysis to the time series considered. Fig. 5 shows a comparison between observations of zonal wind at 55°N and 87.5 km height (courtesy of Werner Singer, 2002) (thin solid line), the MFR daily-mean zonal wind at 8.7° and at 86 km (dotted line), and the daily zonal-mean WINDII temperatures at 5°N–15°N and 86 km height (solid circles). The thick line shows the result of a 7-day smoothing filter applied to the MFR daily-mean zonal wind data for the period of December 1992–March 1993 (Day 335–456). The WINDII temperatures are presented as the difference between the observations and the mean over the period of interest and allow the data comparison on the same scale. As can be seen the zonal winds observed at 55°N and 10°N appear out of phase. The cross-correlation coefficient between the winds at 55°N and 8.7°N was found to be 0.52 with a time lag of 15 days, indicating a delay in the perturbations seen at 8.7°N in comparison with those at 55°N. This time lag is twice as long as that reported by Sivakumar et al. (2004) between high and tropical latitudes during major SSW. The cross-correlation of the MFR winds and the WINDII temperatures at 86 km and 5°N–15°N is −0.57 with a time lag of 8 days, that is the two datasets are out of phase and

the perturbations in the MFR preceded those in the zonal mean temperature by 8 day. The time lag is not surprising considering the fact that the correlation is between zonally averaged daily mean values (the temperatures) and daily mean values (the zonal winds). The cross-correlation was applied only to the period for which there are both wind and temperature data. In addition to the correspondence found between WINDII and MLS daytime observations as seen in Figs. 2 and 3 the cross-correlation between the two datasets at 86 km and over the period of Day 420–456 (late February–March 1993) is 0.72 with a lag of 4 days. Considering the differences in the vertical resolution of the datasets in the upper mesosphere this lag is considered to be insignificant. Table 1 summarises the results of the cross-correlation analysis.

The day/longitude maps of the WINDII temperatures at 86 km (expressed as the residual after the seasonal mean was subtracted from the daily zonal mean), given in Fig. 6 indicates global cooling of the mesosphere following December solstice and continuing for about a month, until Day 390 (January 24, 1993). Another massive cooling takes place around Day 435–456 (March 8–March 31), as the temperatures observed are comparable with those of the summer mesopause at high latitudes, reaching values of the order of −40 K and associated with the coupling of the SAO and the QBO at these latitudes, having its source in the residual circulation at these latitudes (Shepherd et al., 2005, Fig. 8).

The next step in the study is the analysis of the UKMO stratospheric assimilated data at 1 hPa pressure level to examine the large-scale planetary wave activity at 10°N, obtained as an average value of the data at 7.5°N, 10°N, and 12.5°N, for the winter of 1992–1993. Fig. 7 gives the zonally averaged UKMO assimilated temperature, zonal and meridional winds at 10°N and 1 hPa pressure level (∼45 km) for the period from October 1992 to April 1993. There are four events of interest (indicated with arrows in Fig. 7a) in these assimilated fields as follows: (1) In mid-December 1992 a cold temperature anomaly of 4 K from the seasonal mean (Fig. 7a) is accompanied by the zonal mean zonal wind reversal from westerly to easterly, marking the transition from fall to winter (Fig. 7b) and a brief reversal of the meridional wind (Fig. 7c); (2) At the end of January–early February, there is a slight decrease in the zonal mean temperature accompanied by a maximum of the zonal mean easterly wind ($-20\ \mathrm{ms}^{-1}$) and a maximum in the zonal mean northward meridional wind ($4.8\ \mathrm{ms}^{-1}$). After that the zonal mean easterly and northward winds begin weakening with time, throughout most of February; (3–4) A weak warm temperature anomaly (1 K) is observed in mid-February, immediately followed by a cold anomaly in the second half of February which gradually weakens and turns into a warm anomaly in early March, thus marking a temperature change of about 7 K between these two events, and an increase by 4 K above the seasonal mean. In the zonal mean zonal wind there is insignificant and brief increase of the easterly
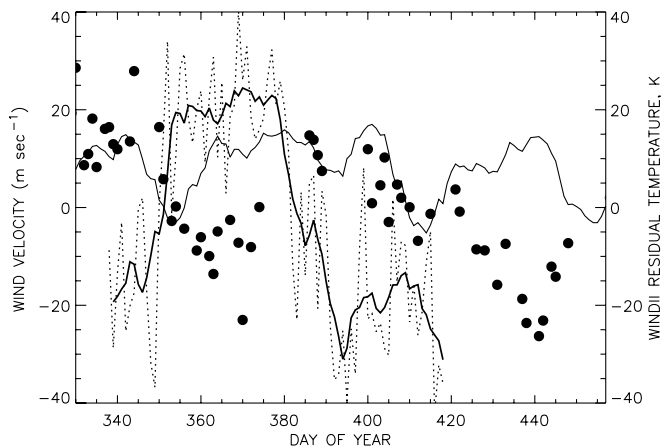
Fig. 5. WINDII temperatures and zonal wind velocities at 86 km for the period from December 1992 to March 1993. The thin solid line gives the zonal wind velocities at 87.5 km altitude and at 55°N (meteor radar at Juliusruh), the dotted line gives the MFR zonal wind velocities at 86 km, along with the 7-day smoothed data (thick solid line) and the WINDII daily zonal mean temperatures at 86 km averaged over the latitude range of 5°–15°N and centred at 10°N (solid circles).

Table 1
Summary of cross-correlation results

Dataset/Experiment	Cross-correlation coefficient	Lag, days
Meteor R (88 km)–MFR (86 km)	0.52	−15
WINDII (86 km)–MFR (86 km)	−0.58	−6
WINDII (86 km)–MFR (80 km)	0.79	−6
WINDII (86 km)–MLS (86 km) February–March 1993	0.72	4
WINDII (86 km)–MLS (50 km) February–March 1993	0.55	4
MLS (86 km)–MLS (50 km) February–March 1993	0.79	0

wind (2 ms^{-1}) at the time of the cold temperature perturbation before reversing to westerly wind in early March, with the time of the zero mean zonal wind coinciding with the time of the warm temperature anomaly at 1 hPa. The zonal mean meridional wind which is northward at the time of the cold temperature perturbation (2 ms^{-1}) decelerates and becomes southward with 1 ms^{-1} before quickly reversing again.

Since the main mechanism for planetary wave amplification with regard to their relationship to SSW, is considered to be the resonant wave (wave 1 and wave 2) amplification under winter conditions (Liu and Roble, 2002, and the references therein) we examine the stationary planetary waves (SPW) with wave-number $m = 1$ and $m = 2$ at 1 hPa pressure level (~45 km) for the 1992–1993 winter season, shown in Fig. 8. Here we are interested in the period of December–March. In the temperature field a stationary wave $m = 1$ and amplitude of 1 K is observed in mid-February (Fig. 8a). In the zonal mean wind SPWs with amplitudes of 6 ms^{-1} and 5 ms^{-1} are detected at the end of January and early March (Fig. 8c), while the largest SPW $m = 1$ in the meridional wind with an amplitude of ~3.5 ms^{-1} is observed in the second half of February and remains relatively strong throughout March 1993 (Fig. 8e) at the time of the cold temperature anomalies

observed in the mesosphere (Figs. 2 and 3a) and the SSW seen in the zonal mean temperatures (Fig. 8a). Another SPW $m = 1$ with 1.8 ms^{-1} is also observed at the end of January 1993. The SPW $m = 2$, shown in Fig. 8b, d, and f generally appear weaker in the temperature and zonal wind assimilated fields, but are still present throughout the entire period with small peaks at the end of January, second half of February and early March. The SWP $m = 2$ in the meridional wind peaks in mid-February and is comparable in amplitude with the SPW $m = 1$.

WINDII TEMPERATURE (K), 86 km, 5N–15N
December 1992 – March 1993
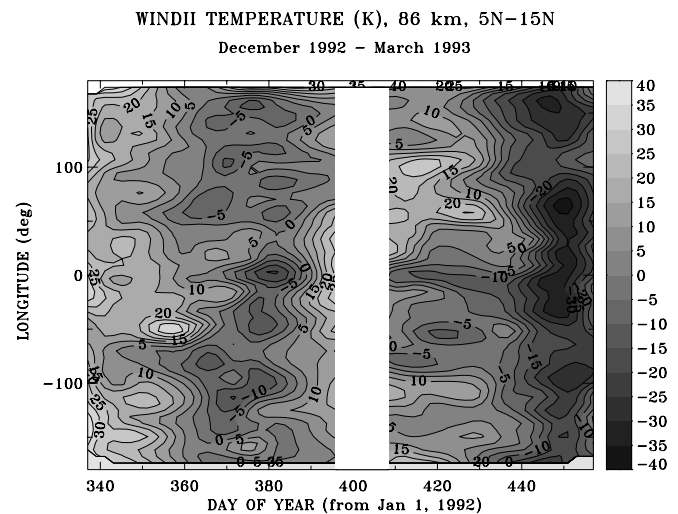
Fig. 6. Time-longitude cross section of the temperature field at 86 km from December 1 1992 to March 31, 1993, as seen by WINDII. The temperature is given as the residual between the observations and the seasonal mean.
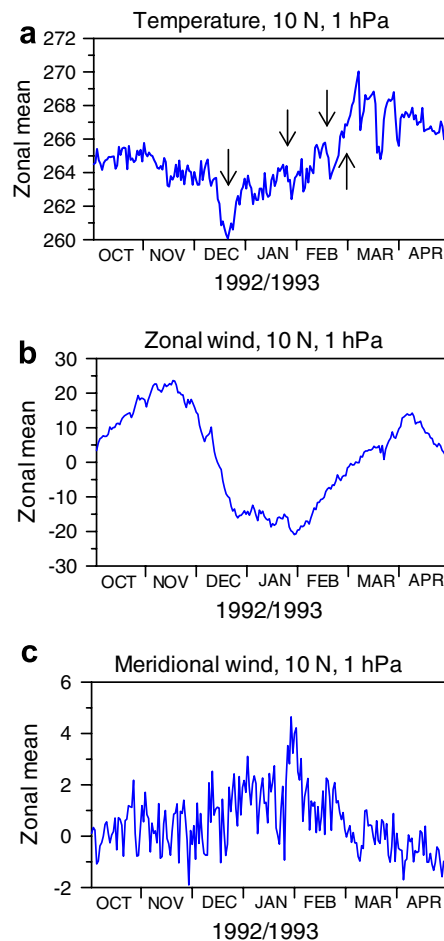
Fig. 7. The UKMO assimilated data for the periods of October 1992 to April 1993 at 10 N and 1 hPa pressure level (~45 km) for the zonal mean fields of: (a) temperature (K); (b) zonal wind (ms^{-1}), and (c) meridional wind (ms^{-1}). The arrows indicate the approximate position of the perturbation to be examined (see text).
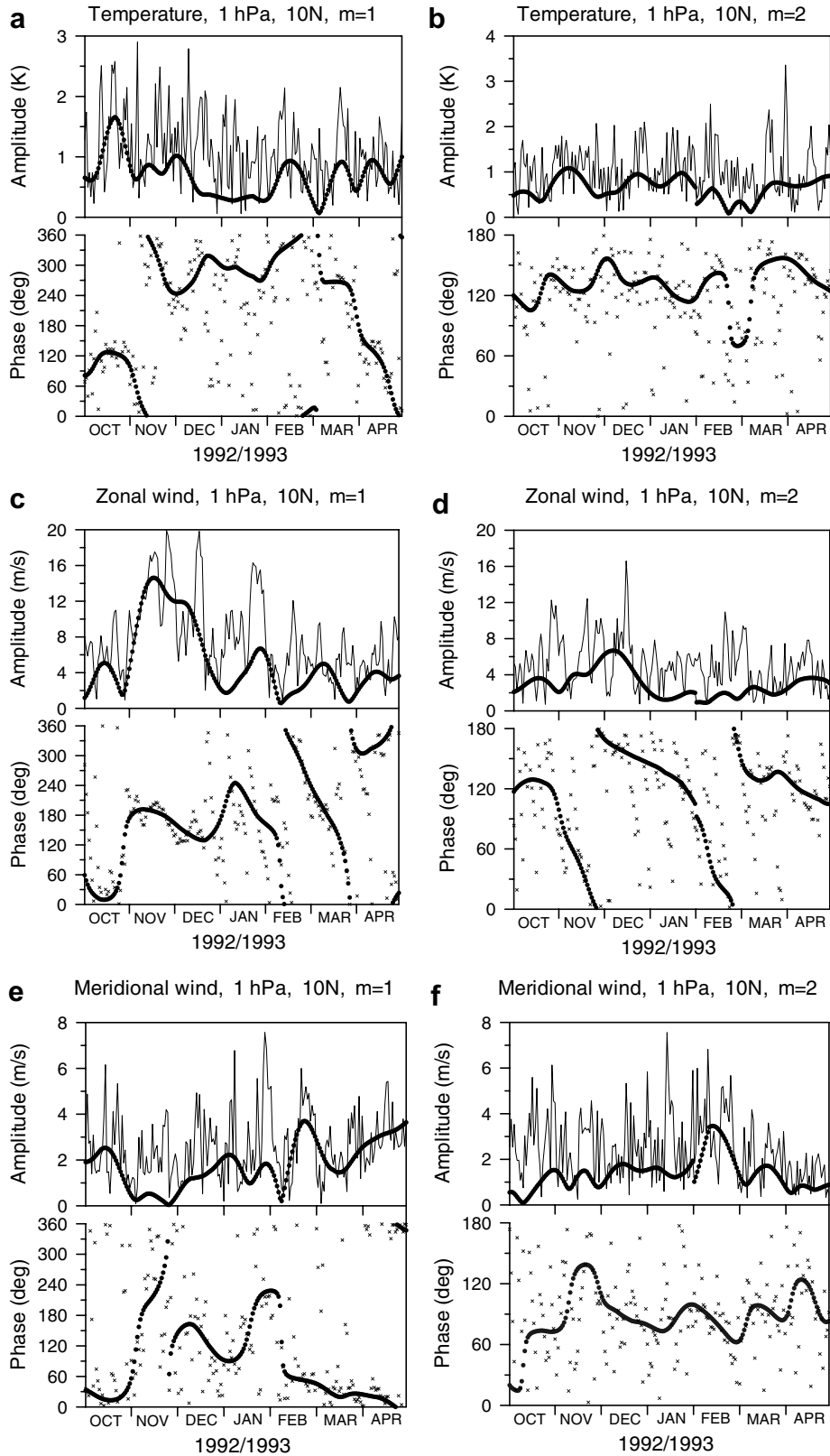
Fig. 8. Amplitudes and phases of planetary stationary (thick solid line) and planetary waves (thin lines) with zonal wave-numbers $m = 1$ (left column) and $m = 2$ (right column) for the period of October 1992–April 1993 at 10°N and 1 hPa pressure level (∼45 km) for the three UKMO assimilated data fields: (a and b) temperature (K); (c and d) zonal wind (ms^{-1}), and (e and f) meridional wind (ms^{-1}), respectively.

Lomb-Scargle periodograms with amplitude and phase determination (Scargle, 1982; Hocke, 1998) and Morlet wavelet (Torrence and Compo, 1998) were derived from the four datasets (WINDII, MLS and MFR at 86 km, the MLS and UKMO at 45–50 km) to study long-period planetary waves present in these observations. Only planetary waves with periods of 2–20 days are considered.

In the stratosphere at 1 hPa (Fig. 9) a dominant temperature westward propagating $m = 1$ wave is detected in mid-December with a period of 7–8 days. The wave appears coupled with a weaker 12–14-day wave while another weak planetary wave signature with a period of 10–17 days is present at the end of February and early March. In general these signatures are weak with amplitudes not exceeding 0.5 K (Fig. 9a). The westward $m = 2$ temperature waves are also weak with a period of 3–4 days at the end of January and the late February, respectively, while a 9–13 days wave extends over February and March, 1993 (Fig. 9b). In the zonal wind the dominant westward propagating $m = 1$ wave has a period of 14 days (4.5 ms^{-1}) with a maximum in mid-January and accompanied by a 7-day wave (3.5 ms^{-1}). Weaker 7–9 day westward $m = 1$ waves are also observed in mid-February and mid-March (Fig. 9c). The amplitude of the observed westward $m = 2$ planetary waves is about a half that for $m = 1$. An 8–9 day wave with amplitude of 2.5 ms^{-1} is observed in mid-December to early February, 1993, while 5–6 day waves are observed in mid-Febru-

ary and early–March together with a 16–18 day wave at the end of February and early March at the time of the SSW observed at mid-latitudes (Fig. 9d).

The temperature eastward propagating planetary waves with $m = 1$, shown in Fig. 10a, are confined to periods of less than 15 days. A 5–10 day wave is present throughout the mid-December–mid-February interval with its period increasing over time. Other 4-day planetary $m = 2$ wave with amplitude of 0.3–0.4 K are detected in January and February, while an 8–15 day wave can be seen at the end of December with a peak period of 11 days (Fig. 10b). A 10–12 day wave is also detected from mid-February through March 1993 (Fig. 10b). There is very weak zonal wind eastward planetary wave activity both for $m = 1$ and $m = 2$ during the period of interest and the respective plots are given in Fig. 10c and d, for completeness.

In the mesosphere the Morlet wavelet analysis of the WINDII temperatures at 86 km, shown in Fig. 11a, reveals the presence of a 4- and 7-day wave around Day 335–345 (December 1–10, 1992) and a 16-day wave with maximum amplitude of 5 K, around winter solstice (Day 355) which extends from ∼Day 360 to Day 380 (December 25–January 15, 1993). Toward mid-January, ∼Day 380, an 8-day wave with amplitude of 4 K is also detected. Another 4-day wave is observed in mid-February while a 14–16 day wave appears again in March 1993 (Day 425–456) (Fig. 11a). These signatures correlate in time with the SSW observed
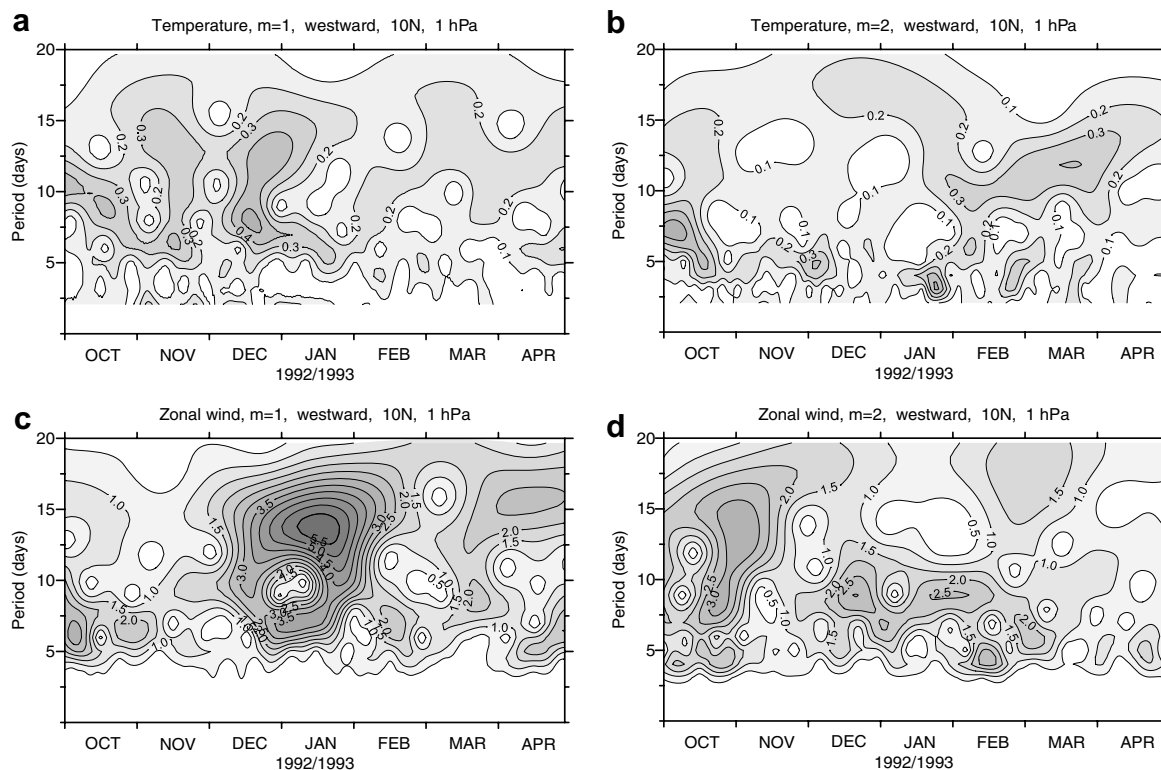
Fig. 9. Wavelet amplitude spectra at 10°N and 1 hPa pressure level (∼45 km) for planetary *westward*-propagating waves with zonal wave-numbers $m = 1$ (left column) and $m = 2$ (right column), for the period of October 1992–April 1993 extracted from the UKMO assimilated fields: (a and b) temperature, (c and d) zonal wind.
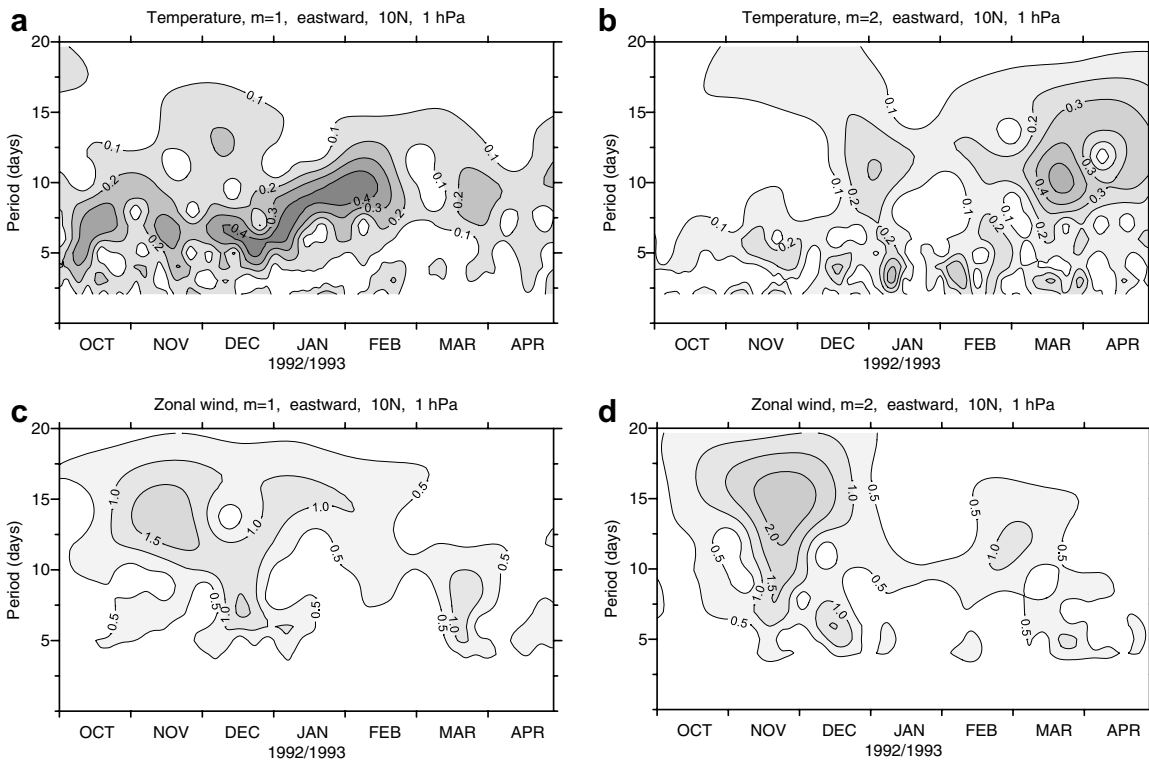
Fig. 10. Wavelet amplitude spectra at 10°N and 1 hPa pressure level (∼45 km) for planetary *eastward*-propagating waves with zonal wave-numbers $m = 1$ (left column) and $m = 2$ (right column), for the period of October 1992–April 1993 extracted from the UKMO assimilated fields: (a and b) temperature, (c and d) zonal wind.

at mid-latitudes (Hoffmann et al., 2002), the cold temperature anomaly seen in the WINDII and MLS data (Figs. 2 and 3a), the stationary planetary waves (Figs. 8c and 9c) and the perturbations in the zonal mean winds already presented. Because there are gaps in the WINDII data no wave structures were observed between Day 380 and 405; no short-period waves were identified, either.

With the MLS data arranged in the same local times as WINDII there is a good correlation between the planetary wave signatures seen in the MLS temperature wavelet at 86 km (Fig. 11b) and those revealed in the WINDII dataset. This similarity can be traced in the signatures from Day 335–380 (December 1992–early January 1993) with a 14-day wave extending through the period (Day 350–380) and accompanied by an 8- and a weaker 4-day waves around Day 370–380 (January 4–14). These signatures appear associated in time with the first cold temperature anomaly seen around Day 360–380 in Figs. 2 and 3a. The remaining period of interest is dominated by a band of 13–18 day wave. The amplitude of the waves identified in the MLS data is about a factor of 2 smaller than those seen in the WINDII dataset.

In the stratosphere at 50 km the planetary wave activity during the Day 360–380 interval (not shown here) appears similar to that already observed in the mesospheric wavelets for WINDII and MLS. The interval is dominated by a planetary wave signature with a period of 10 days, centred at Day 370. Another weaker 5-day wave is also present in early January (∼Day 370) and in the first half of February (Day 400–410). The interval of Day 420–450 when the second cold temperature anomaly is observed in the mesosphere shows the presence of a 16-day wave throughout this interval. These similarities suggest the coupling between the stratosphere and mesosphere as seen in the observations considered.

The MFR zonal wind field from January to mid-February (Day 365–410) at 86 km, shown in Fig. 11c, is dominated by a 10-day wave with a peak of 11 ms^{-1} around Day 390. This is in a very good agreement with the westward $m = 1$ wave with a period of 14 days observed at 1 hPa (Fig. 9c), as well as the stationary $m = 1$ planetary waves in the zonal and meridional winds given in Fig. 8b and c. The strongest signature is a 5-day wave preceding December solstice around Day 350 together with a weaker ∼10-day wave and amplitude of 6 ms^{-1}. Another 13-day wave with amplitude of 6 ms^{-1} can be seen around Day 415.

4. Summary

Preliminary results have been presented on the possible effects of minor SSW events on the tropical mesosphere for the period of December 1992–March 1993 at 5°N–15°N. Four datasets for this period, from WINDII, MLS, MFR and the UKMO were analyzed to examine the temperature and mean zonal wind structure in the mesosphere and their
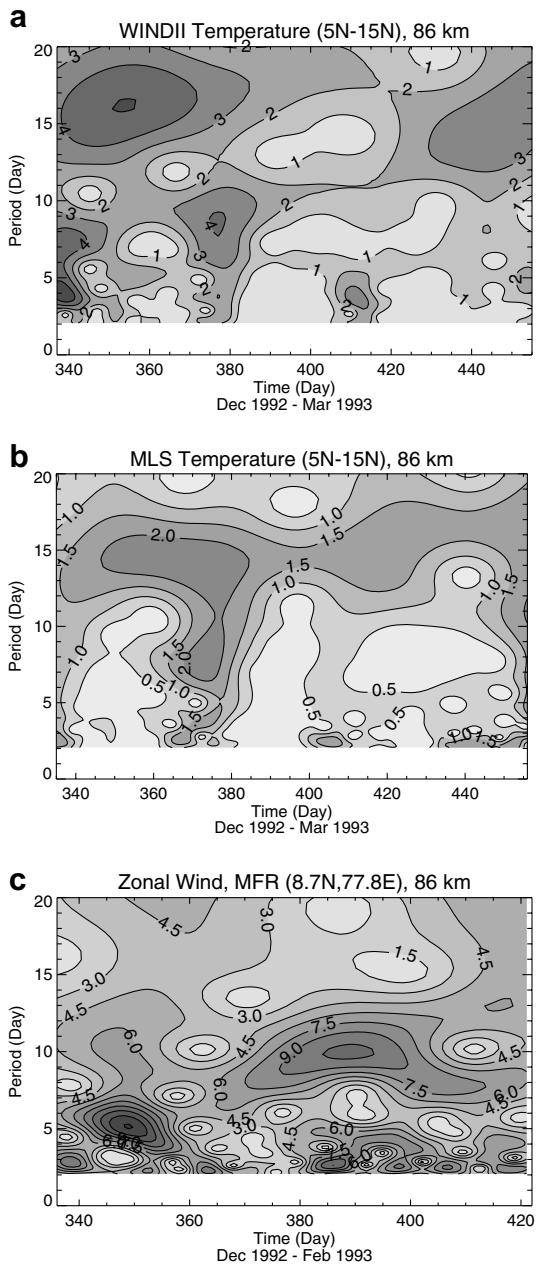
Fig. 11. Morlet wavelet at 86 km from December 1992 to March 1993 of the WINDII (a) and MLS (b) zonal mean temperatures, and from December 1992 to February 1993 of the MFR zonal winds (c) observations.

relationship to perturbations observed in the stratosphere and mid-latitudes. A high degree of correlation was observed between the perturbations at middle and tropical latitudes in the ground-based daily-mean zonal winds between Day 340 and 420, with a time lag of two weeks. Both satellite experiments (WINDII and MLS) indicated cooling in the mesosphere at the time of the stratospheric warming event at the end of February and early March 1993. If we assume that the 15-day delay found in the tropical zonal wind response to the perturbations at mid-latitudes was held beyond Day 420, along with the 6–8 day delay between the response of the tropical zonal mean tem-

perature and that of the daily mean zonal wind, then the response of the tropical mesospheric temperature field to the minor SSW observed on Day 413 (February 16, 1993) at 55°N, expressed as mesospheric cooling would be placed within the period of the cold temperature anomaly around Day 434–436 (March 9–11, 1993) at 5°N–15°N, seen in Figs. 2 and 3a.

The stratospheric temperature increased by 11 K, while the mesosphere cooled by ∼13K during the same period. The spectral analysis applied to the temperature and wind data in the mesosphere revealed the presence of large-scale planetary wave 1 with periods of 4–7 days, 8–12 days and 13–18 days, from which the 13–18 day signature dominated the period of late February–March. At the same time the planetary waves in the stratosphere at 1 hPa appeared to be mostly $m = 2$ with periods of 5- and 9–13 days in the assimilated zonal mean temperature field and 7- and 16–18 days – in the zonal mean zonal winds. The periods obtained are consistent with the planetary waves detected during SSW events at mid- and high latitudes and together with the cold temperature anomalies observed in the mesosphere, the reversal of the zonal mean wind correlated with the peak in the stationary waves in our view present convincing case of the effect of minor SSW on the tropical middle atmosphere.

Acknowledgements

References

Andrews, D.F., Holton, J.R., Leovy, C.B., Middle Atmosphere Dynamics, Academic Press, London, pp. 259–294, 1987.

Baldwin, M.P., Gray, L.J., Dunkerton, T.J., et al. The quasi biennial oscillation. Rev. Geophys. 39, 179–229, 2001.

Barath, F.T., Chavez, M.C., Cofield, R.E., et al. The upper atmosphere research satellite microwave limb sounder instrument. J. Geophys. Res. 98, 10751–10762, 1993.

Cho, Y.-M., Shepherd, G.G., Won, Y.-I., Sargoytchev, S., Brown, S., Solheim, S. MLT cooling during stratospheric warming events. Geophys. Res. Lett. 31, L10104, doi:10.1029/2004GL01955, 2004.

Fedulina, I.N., Pogoreltsev, A.I., Vaughan, G. Seasonal, interannual and short-term variability of planetary waves in Met Office stratospheric assimilated fields. Q. J. R. Meteorol. Soc. 130 (602), 2445–2458, Part A, 2004.

Forbes, J.M., Wu, D. Solar tides as revealed by measurements of mesospheric temperature by the MLS experiments on UARS. J. Atmos. Sci. 63 (7), 1776–1797, 2006.

Fritz, S., Soules, S.D. Large-scale temperature changes in the stratosphere observed from Nimbus III. J. Atmos. Sci. 27, 1091–1097, 1970.

Gray, L.J., Phipps, S.J., Dunkerton, T.J., Baldwin, M.P., Drysdale, E.F., Allen, M.R. A data study of the influence of the equatorial upper

stratospghere on northern- hemisphere stratospheric warmings. Q. J. R. Meteorol. Soc. 127, 1985–2003, 2001.

Gregory, J.B., Manson, A.H. Winds and wave motions to 110 km at mid-latitudes. III. response of mesospheric and thermospheric winds to major stratospheric warmings. J. Atmos. Sci. 32, 1676–1681, 1975.

Hirota, I., Barnett, J. Planetary waves in the winter mesosphere – preliminary analysis of Nimbus 6 PMR results. Q. J. R. Meteorol. Soc. 103, 487–498, 1977.

Hocke, K. Phase estimation with the Lomb-Scargle periodogram method. Ann. Geophys. 16, 356–358, 1998.

Hoffmann, P., Singer, W., Keuer, D. Variability of the mesospheric wind field at middle and Arctic latitudes in winter and its relation to stratospheric circulation disturbances. J. Atmos. Solar-Terr. Phys. 64, 1229–1240, 2002.

Kodera, K. Influence of stratospheric sudden warming on the equatorial troposphere. Geophys. Res., Lett. 33, L06804, doi:10.1029/2005GL02451, 2006.

Labitzke, K. Temperature channels in the mesosphere and stratosphere connected with circulation changes in winter. J. Atmos. Sci. 29, 756–766, 1972.

Labitzke, K. Sunspots, the QBO and the stratospheric temperature in the north polar region. Geophys. Res. Lett 14, 535–537, 1987.

Labitzke, K., Naujokat, B. The lower Arctic stratosphere in winter since 1952, SPARC Newsletter 15, 2000.

Lieberman, R.S., Riggin, D. High resolution Doppler imager observations of Kelvin waves in the equatorial mesosphere and lower thermosphere. J. Geophys. Res. 102, 26117–26130, 1997.

Liu, H.-L., Roble, R.G. A study of a self-generated stratospheric sudden warming and its mesospheric-lower thermospheric impacts using the coupled TIME-GCM/CCM3. J. Geophys. Res. 107 (D23), 4695, doi:10.1029/2001JD00153, 2002.

Manson, A.H., Meek, C., Chshyolkova, T., et al. Winter warmings, tides and planetary waves: comparisons between CMAM (with interactive chemistry) and MFR-MetO observations and data. Ann. Geophys. 24, 1–26, 2006.

Matsuno, T. A dynamical model of the stratospheric sudden warming. J. Atmos. Sci. 28, 1479–1494, 1971.

Meriwether, J.W., Gao, X., Wickwar, V.B., Wilkerson, T., Beissner, K., Collins, S., Hagan, M.H. Observed coupling of the mesosphere inversion layer to the thermal tidal structure. Geophys. Res. Lett. 25 (9), 1479–1482, 1998.

Mukherjee, B.K., Ramana Murty, Bh.V. High-level warmings over a tropical station. Mon. Weather Rev. 100 (9), 674–681, 1972.

Mukherjee, B.K., Indira, K., Dani, K.K. Perturbations in tropical middle atmosphere durng winter, 1984–1985. Meteorol. Atmos. Phys. 37, 17–26, 1987.

Orsolini, Y.J., Limpasuvan, V., Leovy, C. The tropical stratopause in the UKMO stratospheric analyses: Evidence for a 2-day wave and inertial circulation. Q. J. R. Meteorol. Soc. 123, 1707–1724, 1997.

Quiroz, R.S. The warming of the upper stratosphere in February 1966 and the associated structure of the mesosphere. Mon. Weather Rev. 97 (8), 541–552, 1969.

Quiroz, R.S. The determination of the amplitude and altitude of stratospheric warming from satellite-measured radiance change. J. Appl. Meteorol. 10 (3), 555–574, 1971.

Rajaram, R., Gurubaran, S. Seasonal variabilities of low-latitude mesospheric winds. Ann. Geophys. 16, 197–204, 1998.

Reber, C.A., Trevathan, E.C., O'Neal, J.R., Luther, R.M. Upper Atmosphere Research Satellite (UARS) mission. J. Geophys. Res. 98, 10643–10647, 1993.

Scargle, J.D. Studies in aeronomical time series analysis: II. Statistical aspects of spectral analysis of unevenly spaced data. Astrophys. J. 263, 835–853, 1982.

Shepherd, G.G., Thuillier, G., Gault, W.A., et al. WINDII, the wind imaging interferometer on the Upper Atmosphere Research satellite. J. Geophys. Res. 98, 10725–10750, 1993.

Shepherd, M.G., Reid, B., Zhang, S.P., Solheim, B.H., Shepherd, G.G., Wickwar, V.B., Herron, J.P. Retrieval and validation of mesospheric temperatures from Wind Imaging Interferometer observations. J. Geophys. Res. 106, 24813–24829, 2001.

Shepherd, M.G., Evans, W.J.F., Hernandez, G., Offermann, D., Takahashi, H. Global variability of mesospheric temperature: Mean temperature field. J. Geophys. Res. 109 (D24), D24117, doi:10.1029/2004JD00505, 2004.

Shepherd, M.G., Shepherd, G.G., Evans, W.F.J., Sridharan, S. Global variability of mesospheric temperature: Planetary scale perturbations at equatorial and tropical latitudes. J. Geophys. Res. 110 (D24), D24103, doi:10.1029/2005JD00612, 2005.

Shepherd, M.G., Wu, D.L. Fedulina, I.N., Gurubaran, S., Russell, J.M., Mlynczak, M.G., Shepherd, G.G. Stratospheric warming effects on the tropical mesospheric temperature field, J. Atmos. Solar-Terr. Phys., in press, doi:10.1016/j.jastp.2007.04.009, 2007.

Sivakumar, V., Morel, B., Bencherif, H., Baray, J.L., Baldy, S., Hauchecorne, A., Rao, P.B. Rayleigh lidar observation of a warm stratopause over a tropical site, Gadanki (13.5°N, 79.2°E). Atmos. Chem. Phys. 4, 1989–1996, 2004.

Swinbank, R., O'Neill, A. A stratosphere-troposphere data assimilation system. Mon. Weather Rev. 122, 686–702, 1994a.

Swinbank, R., O'Neill, A. Quasi-biennial and semi-annual oscillations in equatorial wind fields constructed by data assimilation. Geophys. Res. Lett. 21, 2099–2102, 1994b.

Swinbank, R., Ortland, D.A. Compilation of wind data for the Upper Atmosphere Research Satellite (UARS) Reference Atmosphere Project. J. Geophys. Res. 108 (D19), 4615, 1029/2002JD00313, 2003.

Torrence, Ch., Compo, G.P. A practical guide to wavelet analysis. Bull. Am. Meteorol. Soc. 79 (1), 61–78, 1998.

Vincent, R.A., Lesicar, D. Dynamics of the equatorial mesosphere: First results with a new generation partial reflection radar. Geophys. Res. Lett. 18, 825–828, 1991.

Walterscheid, R.L., Sivjee, G.G., Roble, R.G. Mesopsheric and lower thermospheric manifestations of a stratospheric warming event over Eureka, Canada (80°N). Geophys. Res. Lett. 27 (18), 2897–2900, 2000.

Whiteway, J.A., Carswell, A.I. Rayleigh lidar observations of thermal structure and gravity wave activity in the high arctic during a stratospheric warming. J. Atmos. Sci. 51, 3122–3136, 1994.

Wu, D.L., Read, W.G., Shippony, Z., Leblanc, T., Duck, T.J., Ortland, D.A., Sica, R.J., Argall, P.S., Oberheide, J., Hauchecorne, A., Keckhut, P., She, C.Y., Krueger, D.A. Mesospheric temperature from UARS MLS: retrieval and validation. J. Atmos. Solar-Terr. Phys. 65, 245–267, 2003.